

Regime of Validity of Sound-Proof Atmospheric Flow Models

RUPERT KLEIN

Mathematik & Informatik, Freie Universität Berlin, Germany

*

ULRICH ACHATZ

Meteorologie, Goethe-Universität, Frankfurt, Germany

DIDIER BRESCH

LAMA, CNRS, Université de Savoie, Chambéry, France

OMAR M. KNIO

Mechanical Engineering, The Johns Hopkins University, Baltimore, MD, USA

PIOTR K. SMOLARKIEWICZ

NCAR, Bolder, CO, USA

* *Corresponding author address:* Rupert Klein, FB Mathematik & Informatik, Freie Universität Berlin,

Arnimallee 6, 14195 Berlin, Germany. E-mail: rupert.klein@math.fu-berlin.de

ABSTRACT

Ogura and Phillips (1962) derived their original anelastic model through systematic formal asymptotics using the flow Mach number as the expansion parameter. To arrive at a reduced model which would simultaneously represent internal gravity waves and the effects of advection, they had to adopt a distinguished limit stating that the dimensionless stability of the background state be of the order of the Mach number squared. For typical flow Mach numbers of $M \sim 1/30$ this amounts to total variations of potential temperature across the troposphere of less than one Kelvin, i.e., to unrealistically weak stratification. Various generalizations of Ogura and Phillips' anelastic model have been proposed to remedy this issue, e.g., by Dutton & Fichtl (1969), and Lipps & Hemler (1982). Following the same goals, but a somewhat different route of argumentation, Durran proposed the pseudo-incompressible model in 1989. The present paper provides a scale analysis showing that the regime of validity of two of these extended models covers stratification strengths of order $(h_{\text{sc}}/\theta) d\theta/dz < M^{2/3}$ which corresponds to realistic variations of potential temperature, θ , across the pressure scale height, h_{sc} , of $\Delta\theta \Big|_0^{h_{\text{sc}}} < 30$ K.

1. Introduction

Ogura and Phillips (1962) derived their original anelastic model through systematic formal asymptotics using the flow Mach number as the expansion parameter. To arrive at a reduced model which would simultaneously represent internal gravity waves and the effects of advection, they had to adopt a distinguished limit stating that the dimensionless stability of the background state be of the order of the Mach number, ε , squared. To recall the relevant line of thought, consider Table 1 (after Klein 2009). The left column in that table displays the inverse characteristic timescales of advection, sound propagation, and internal waves. The right column shows these frequencies non-dimensionalized by the advection time scale.

By design, the sound-proof models should be able to address deep atmospheres vertically covering a typical pressure scale height, $h_{\text{sc}} \sim 10$ km, or more, and non-hydrostatic flow regimes corresponding to horizontal scales down to 10 km or less, (cf., Bannon 1996). Thus the characteristic vertical as well as horizontal length scales for the design regime of these models are comparable to the pressure scale height, h_{sc} . As can be seen in Table 1, the characteristic acoustic timescale, t_{ac} , is small of order $O(\varepsilon)$ relative to the advection time, t_{adv} , whereas the timescale for internal waves, t_{int} , i.e., the inverse of the Brunt-Väisälä frequency, N , is of order $O\left(\varepsilon \left[(h_{\text{sc}}/\theta) d\theta/dz\right]^{-1/2}\right)$. As a consequence, if we follow Ogura and Phillips (1962) and construct an asymptotic single timescale model which resolves the advection time scale and includes internal waves at the same time, we would have to adopt a weak stratification so that $(h_{\text{sc}}/\theta) d\theta/dz = O(\varepsilon^2)$.

For typical flow Mach numbers of $M \sim 1/30$ such stratifications amount to total varia-

tions of potential temperature across the troposphere of less than one Kelvin, i.e., to unrealistically weak stratification. Various generalizations of Ogura and Phillips' anelastic model have been proposed to remedy this issue, e.g., by Dutton and Fichtl (1969), Lipps and Hemler (1982), and Bannon (1996). Following the same goals but a somewhat different route of argumentation, Durran (1989) proposed the pseudo-incompressible model.

According to Table 1, however, any such stronger stratification with

$$\frac{h_{\text{sc}}}{\theta} \frac{d\theta}{dz} = O(\varepsilon^\mu) \quad \text{where} \quad 0 < \mu < 2 \quad (1)$$

will induce a three-timescale asymptotic limit so that

$$t_{\text{ac}} \ll t_{\text{int}} \ll t_{\text{adv}} \quad \text{with} \quad t_{\text{ac}} = O(\varepsilon t_{\text{adv}}), \quad t_{\text{int}} = O(\varepsilon^{1-\mu/2} t_{\text{adv}}). \quad (2)$$

Sound-proof models derived for such a regime of stratifications will thus constitute asymptotic two-scale models in time, retaining a scale separation between the internal and advection timescales. In deriving their models, Dutton and Fichtl (1969), Lipps and Hemler (1982), Durran (1989), and Bannon (1996) provide a range of physical arguments for their validity. Yet, this inherent multiscale nature of the resulting sound-proof models for stratifications within the regime from (1) is not addressed. We have not found it addressed either in later scaling or asymptotic analyses, such as (Davies et al. 2003; Almgren et al. 2006). At the same time, numerical experience indicates that sound-proof models work well on a much broader range of scales and problems than would be anticipated based on theoretical arguments (cf. Prusa et al. 2008, and references therein).

The presence of multiple scales in the sound-proof models is, nevertheless, an issue, because both the spatial structures and frequencies of internal waves featured by the sound-proof models only approximate those represented by the full compressible flow equations. As

a consequence, there are two necessary conditions for the validity of the sound-proof models over the targeted advective timescales, viz.

- (a) the spatial structures of corresponding internal wave eigenmodes of the sound-proof and compressible systems should be asymptotically close as $\varepsilon \rightarrow 0$, and
- (b) the accumulation of phase differences between such sound-proof and compressible internal waves should remain asymptotically small at least over the advective timescale.

Motivated by these considerations, we consider in this paper atmospheres with stratifications in the regime from (1) and:

- i. compare the internal wave eigenmode structures of the compressible Euler equations and selected sound-proof models;
- ii. assess the approximation errors due to “sound-proofing” for both the spatial eigenmodes and the associated frequencies in terms of the Mach number, and;
- iii. demonstrate, as our main result, that internal wave solutions of the sound-proof and compressible models remain asymptotically close for $t = O(t_{\text{adv}})$ for sufficiently weak stratification. Specifically, for both Lipps & Hemler’s and Durran’s sound-proof models the corresponding bound on the stratification is

$$\frac{h_{\text{sc}}}{\theta} \frac{d\theta}{dz} = O(\varepsilon^\mu) \quad \text{with} \quad \mu > \frac{2}{3}. \quad (3)$$

This corresponds to realistic stratifications with $\Delta\theta \big|_0^{h_{\text{sc}}} = 30\dots 50$ K over 10...15 km.

The rest of the paper is organized as follows. In section 2 we summarize the model equations to be studied. In section 3 we introduce a new set of variables which explicitly reveal the

multiscale nature of fully compressible flows within the regime of stratifications from (1). In section 4, using formal asymptotic analysis and vertical mode decompositions, we compare the vertical internal wave eigenmodes and eigenfrequencies for the pseudo-incompressible and the Lipps & Hemler anelastic models with those of the compressible equations and show that they are asymptotically close as long as $(h_{sc}/\theta) d\theta/dz = O(\varepsilon^\mu)$ for any $\mu > 0$. In that section we also assess the time it takes compressible and sound-proof internal waves to accumulate leading-order deviations of their phases due to these differences in the dispersion relations, and this will lead to the above-mentioned principal result in (3). In section 5 we draw conclusions and provide an outlook to future work.

2. Compressible and sound-proof model equations

The exposition in this section of the three sets of model equations to be analysed subsequently closely follows Klein (2009). Here, we restrict our considerations to flows under gravity, but without Coriolis effects and non-resolved-scale closures, and present consistent dimensionless forms of the compressible Euler equations and of two sound-proof models.

a. Compressible Euler equations

$$\begin{aligned}
 \rho_t + \nabla \cdot (\rho \mathbf{v}) &= 0 \\
 (\rho \mathbf{v})_t + \nabla \cdot (\rho \mathbf{v} \circ \mathbf{v}) + P \nabla \pi &= -\rho \mathbf{k} \ , \\
 P_t + \nabla \cdot (P \mathbf{v}) &= 0
 \end{aligned}
 \tag{4}$$

where (ρ, \mathbf{v}) are the density and flow velocity, $P = p^{1/\gamma} = \rho\theta$ is a modified thermodynamic pressure variable, θ the potential temperature, and $\pi = p^\Gamma/\Gamma$ where $\Gamma = (\gamma - 1)/\gamma$, and γ is the isentropic exponent. Let an asterisk, for the moment, denote dimensional variables, then the dimensionless quantities appearing in (4) are defined as

$$t = \frac{t^* c_{\text{ref}}}{h_{\text{sc}}}, \quad \mathbf{x} = \frac{\mathbf{x}^*}{h_{\text{sc}}}, \quad \rho = \frac{\rho^*}{\rho_{\text{ref}}}, \quad p = \frac{p^*}{p_{\text{ref}}}, \quad \mathbf{v} = \frac{\mathbf{v}^*}{c_{\text{ref}}}, \quad \rho\theta = p^{1/\gamma}, \quad (5)$$

where $c_{\text{ref}} = \sqrt{p_{\text{ref}}/\rho_{\text{ref}}}$ and $h_{\text{sc}} = p_{\text{ref}}/\rho_{\text{ref}} g$, and where p_{ref} , ρ_{ref} , and g denote the sea-level pressure, the corresponding density at a temperature of 300 K, say, and the acceleration of gravity, respectively.

b. Pseudo-incompressible model

If we refrain, in contrast to Durran (1989), from subtracting the background hydrostatic balance from the vertical momentum equation, then the pseudo-incompressible model is obtained from (4) by simply dropping the pressure time derivative and assuming P to match a prescribed background distribution $P \equiv \bar{P}(z)$. Thus we find

$$\begin{aligned} \rho_t + \nabla \cdot (\rho \mathbf{v}) &= 0 \\ (\rho \mathbf{v})_t + \nabla \cdot (\rho \mathbf{v} \circ \mathbf{v}) + \bar{P} \nabla \pi &= -\rho \mathbf{k} \cdot \end{aligned} \quad (6)$$

$$\nabla \cdot (\bar{P} \mathbf{v}) = 0$$

c. Anelastic model

Bannon (1996) discusses various versions of anelastic models which differ from the pseudo-incompressible one in that they adopt the mass conservation law to impose the sound-

removing velocity divergence constraint instead of the pressure equation. The generic anelastic model proposed by Bannon (also Lipps and Hemler (1982)), to be analyzed below, is obtained from (4) by dropping the density time derivative, assuming the density to equal some prescribed background distribution, $\rho \equiv \bar{\rho}(z)$, and by slightly modifying the pressure gradient and gravity terms. With these modifications, we obtain

$$\begin{aligned} \nabla \cdot (\bar{\rho} \mathbf{v}) &= 0 \\ (\bar{\rho} \mathbf{v})_t + \nabla \cdot (\bar{\rho} \mathbf{v} \circ \mathbf{v}) + \bar{\rho} \nabla \pi' &= -\bar{\rho} \frac{\theta - \bar{\theta}}{\bar{\theta}} \mathbf{k} . \end{aligned} \quad (7)$$

$$(\bar{\rho} \theta)_t + \nabla \cdot (\bar{\rho} \theta \mathbf{v}) = 0$$

In all three cases, $\bar{\theta}(z)$ is the mean background potential temperature distribution which defines the background pressure variable, $\bar{P}(z)$, and the background density, $\bar{\rho}(z)$, via $d\bar{p}/dz = -\bar{\rho}g$, $\bar{p}(0) = 1$, $\bar{\rho}\bar{\theta} = \bar{P}$, and $\bar{P} \equiv \bar{p}^{1/\gamma}$. For later reference we note the exact solution,

$$\bar{p}(z) = \bar{P}(z)^\gamma = [\Gamma \bar{\pi}(z)]^{\frac{1}{\Gamma}} , \quad \bar{\rho}(z) = \bar{P}(z)/\bar{\theta}(z), \quad \text{where} \quad \bar{\pi}(z) = \frac{1}{\Gamma} - \int_0^z \frac{1}{\bar{\theta}(\zeta)} d\zeta . \quad (8)$$

We also note that π' in (7) is defined as

$$\pi' = \frac{p - \bar{p}}{\bar{\rho}} , \quad (9)$$

i.e., it is a density-scaled perturbation of the pressure, p , but not of the Exner pressure, π .

3. Scaled variables

The following transformation of variables will explicitly reveal the asymptotic scalings to be discussed in the sequel. First we introduce a time coordinate nondimensionalized by the

characteristic advection time

$$\tau = \varepsilon t \quad (10)$$

and then we let

$$\begin{aligned} \theta(t, \mathbf{x}, z; \varepsilon) &= 1 + \varepsilon^\mu \bar{\Theta}(z) + \varepsilon^{\mu+\nu} \tilde{\theta}(\tau, \mathbf{x}, z; \varepsilon) & (\nu = 1 - \mu/2) \\ \pi(t, \mathbf{x}, z; \varepsilon) &= \bar{\pi}(z) + \varepsilon \tilde{\pi}(\tau, \mathbf{x}, z; \varepsilon) \\ \mathbf{v}(t, \mathbf{x}, z; \varepsilon) &= \varepsilon \tilde{\mathbf{v}}(\tau, \mathbf{x}, z; \varepsilon) \end{aligned} \quad (11)$$

The velocity, \mathbf{v} , was nondimensionalized by $\sqrt{p_{\text{ref}}/\rho_{\text{ref}}}$, which is comparable to the sound speed; whereupon the scaling in (11)₃ implies low Mach number flow when $\varepsilon \ll 1$. The representation of the background potential temperature stratification,

$$\bar{\theta}(z) = 1 + \varepsilon^\mu \bar{\Theta}(z), \quad (12)$$

follows from the stratification regime in (1). The exponent ν determines the scaling of the dynamic potential temperature perturbations. Its specific value as given in (11)₁ implies the correct scaling for internal gravity waves as we will see shortly. Furthermore, $\bar{\pi}(z)$ denotes the background Exner pressure distribution given the stratification from (1). We assume a pressure perturbation amplitude of the order of the Mach number, $O(\varepsilon)$, so as to not preclude leading-order acoustic modes at this stage.

For compressible flows, the new variables $\tilde{\theta}, \tilde{\pi}, \tilde{\mathbf{v}}$ satisfy

$$\begin{aligned} \tilde{\theta}_\tau + \frac{1}{\varepsilon^\nu} \tilde{w} \frac{d\bar{\Theta}}{dz} &= -\tilde{\mathbf{v}} \cdot \nabla \tilde{\theta} \\ \tilde{\mathbf{v}}_\tau - \frac{1}{\varepsilon^\nu} \frac{\tilde{\theta}}{\bar{\theta}} \mathbf{k} + \frac{1}{\varepsilon} (1 + \varepsilon^\mu \bar{\Theta}) \nabla \tilde{\pi} &= -\tilde{\mathbf{v}} \cdot \nabla \tilde{\mathbf{v}} - \varepsilon^{1-\nu} \tilde{\theta} \nabla \tilde{\pi} \\ \tilde{\pi}_\tau + \frac{1}{\varepsilon} \left(\gamma \Gamma \bar{\pi} \nabla \cdot \tilde{\mathbf{v}} + \tilde{w} \frac{d\bar{\pi}}{dz} \right) &= -\tilde{\mathbf{v}} \cdot \nabla \tilde{\pi} - \gamma \Gamma \tilde{\pi} \nabla \cdot \tilde{\mathbf{v}} \end{aligned} \quad (13)$$

These equations are obtained from a straightforward *equivalent* transformation of the compressible flow equations in (4) without any asymptotic simplifications.

Besides the tendencies of temporal change, there are three groups of terms in (13): the terms multiplied by $\varepsilon^{-\nu}$ induce internal waves, the terms multiplied by ε^{-1} represent the acoustic modes, and the terms on the right hand side cover all nonlinearities. In fact, all terms on the left hand sides are linear in the unknowns. Notice that all terms on the right are non-singular as $\varepsilon \rightarrow 0$, i.e., they are $O(\varepsilon^\alpha)$ with $\alpha \geq 0$. This clean Mach number scaling of acoustic, internal wave, and nonlinear (advective) terms justifies in hindsight the choice $\nu = 1 - \mu/2$ introduced earlier.

In the new variables the pseudo-incompressible model reads

$$\begin{aligned} \tilde{\theta}_\tau + \frac{1}{\varepsilon^\nu} \tilde{w} \frac{d\bar{\Theta}}{dz} &= -\tilde{\mathbf{v}} \cdot \nabla \tilde{\theta} \\ \tilde{\mathbf{v}}_\tau - \frac{1}{\varepsilon^\nu} \frac{\tilde{\theta}}{\bar{\theta}} \mathbf{k} + \frac{1}{\varepsilon} (1 + \varepsilon^\mu \bar{\Theta}) \nabla \tilde{\pi} &= -\tilde{\mathbf{v}} \cdot \nabla \tilde{\mathbf{v}} - \varepsilon^{1-\nu} \tilde{\theta} \nabla \tilde{\pi} , \\ &\left(\gamma \Gamma \bar{\pi} \nabla \cdot \tilde{\mathbf{v}} + \tilde{w} \frac{d\bar{\pi}}{dz} \right) = 0 \end{aligned} \quad (14)$$

whereas the anelastic model becomes

$$\begin{aligned} \tilde{\theta}_\tau + \frac{1}{\varepsilon^\nu} \tilde{w} \frac{d\bar{\Theta}}{dz} &= -\tilde{\mathbf{v}} \cdot \nabla \tilde{\theta} \\ \tilde{\mathbf{v}}_\tau - \frac{1}{\varepsilon^\nu} \frac{\tilde{\theta}}{\bar{\theta}} \mathbf{k} + \frac{1}{\varepsilon} \nabla \tilde{\pi} &= -\tilde{\mathbf{v}} \cdot \nabla \tilde{\mathbf{v}} . \\ - \varepsilon^\mu \frac{\gamma \Gamma \bar{\pi}}{\bar{\theta}} \tilde{w} \frac{d\bar{\Theta}}{dz} + \left(\gamma \Gamma \bar{\pi} \nabla \cdot \tilde{\mathbf{v}} + \tilde{w} \frac{d\bar{\pi}}{dz} \right) &= 0 \end{aligned} \quad (15)$$

We observe that the potential temperature transport equations are in agreement between all three models. This was to be expected as in the present adiabatic setting, this equation reduces to a simple advection equation. The momentum equations of the compressible and pseudo-incompressible models are in complete agreement, whereas the anelastic model's

momentum equation lacks the terms responsible for baroclinic vorticity production. These are the respective last terms on the left and right from (13)₂ or (14)₂, which combine to yield $\varepsilon^{\mu-1} \left(\bar{\Theta} + \varepsilon^\nu \tilde{\theta} \right) \nabla \tilde{\pi}$.¹

The only difference between the compressible Euler equations from (13) and the pseudo-incompressible model is found in the Exner pressure evolution equation, (13)₃, which becomes the pseudo-incompressible divergence constraint in (14)₃. The anelastic divergence constraint in (15)₃ again differs from the pseudo-incompressible one through an additional term involving the background potential temperature stratification.

4. Internal gravity waves

a. Gravity wave scaling

The compressible flow equations from (13) feature three distinct time scales for sound propagation, $\tau = O(\varepsilon)$, for internal waves, $\tau = O(\varepsilon^\nu)$, and for advection, $\tau = O(1)$. In this section we consider solutions that do not feature sound waves but evolve on time scales comparable to the internal wave time scale. The only “sound-term” of order $O(\varepsilon^{-1})$ in the momentum equation is the one involving the pressure gradient. This term will reduce to order $O(\varepsilon^{-\nu})$, and thus induce changes on the internal wave time scale only, provided that the pressure perturbations satisfy $\tilde{\pi} = \varepsilon^{1-\nu} \pi^*$ with $\pi^* = O(1)$. By introducing this additional rescaling of the pressure fluctuations and by adopting an internal wave time coordinate $\vartheta = \varepsilon^{-\nu} \tau$, the compressible, pseudo-incompressible, and anelastic systems can be

¹Notice that $\mu - 1 + \nu = 2(1 - \nu) - 1 + \nu = 1 - \nu$.

represented as

$$\begin{aligned}
\tilde{\theta}_\vartheta + \tilde{w} \frac{d\bar{\Theta}}{dz} &= -\varepsilon^\nu \tilde{\mathbf{v}} \cdot \nabla \tilde{\theta} \\
\tilde{\mathbf{v}}_\vartheta - \frac{\tilde{\theta}}{\bar{\theta}} \mathbf{k} + (1 + B \varepsilon^\mu \bar{\Theta}) \nabla \pi^* &= -\varepsilon^\nu \tilde{\mathbf{v}} \cdot \nabla \tilde{\mathbf{v}} - B \varepsilon^{\mu+\nu} \tilde{\theta} \nabla \pi^* \quad , \\
A \varepsilon^\mu \pi_\vartheta^* - C \varepsilon^\mu \frac{\gamma \Gamma \bar{\pi}}{\bar{\theta}} \tilde{w} \frac{d\bar{\Theta}}{dz} + \left(\gamma \Gamma \bar{\pi} \nabla \cdot \tilde{\mathbf{v}} + \tilde{w} \frac{d\bar{\pi}}{dz} \right) &= -A \varepsilon^{\mu+\nu} (\tilde{\mathbf{v}} \cdot \nabla \pi^* + \gamma \Gamma \pi^* \nabla \cdot \tilde{\mathbf{v}})
\end{aligned} \tag{16}$$

with the choices of the switching parameters as summarized in Table 2.

We observe that in the gravity wave scaling all differences between the compressible model on the one hand and both of the sound-proof models on the other hand are of order $O(\varepsilon^\mu)$ or smaller, i.e., at least of the order of the stratification strength. At leading order in ε , all models agree from a formal scaling perspective, although switching off the pressure tendency by letting $A = 0$ fundamentally changes the mathematical type of the equations from strictly hyperbolic to mixed hyperbolic-elliptic. We will demonstrate below through formal asymptotics that this, nevertheless, affects the internal gravity wave solutions only weakly. Between the pseudo-incompressible and anelastic systems there is no such singular switch, however, so that their solutions will differ only by $O(\varepsilon^\mu)$ at least on internal wave time scales with $\vartheta = O(1)$.

b. The constraint on the stratification

The leading perturbation terms in (16) involve terms of order $O(\varepsilon^\mu)$ in the linearized part on the left, and terms of order $O(\varepsilon^\nu)$ in the nonlinear part of the equations on the right. This suggest that for $\mu < \nu$, i.e., for $\varepsilon^\mu \gg \varepsilon^\nu$, the linearized internal wave eigenmodes and eigenvalues of the three systems differ by $O(\varepsilon^\mu)$ only, and nonlinear effects will contribute

merely even higher-order perturbations. In this setting, we may expect solutions of the three models that start from comparable internal wave initial data to remain close with differences of order $O(\varepsilon^\mu)$ over the internal wave time scale with $\vartheta = O(1)$. Yet, we are really interested in flow evolutions over advective time scales with $\tau = \varepsilon^\nu \vartheta = O(1)$. Over such longer time scales, the expected differences in the internal wave eigenfrequencies of order $O(\varepsilon^\mu)$ will accumulate to phase shifts of order $\varepsilon^\mu \cdot \vartheta = O(\tau \cdot \varepsilon^{\mu-\nu}) = O(\varepsilon^{\mu-\nu})$. As a consequence, the linearized internal wave solutions of the three models should remain asymptotically close even over advective time scales provided

$$\varepsilon^{\mu-\nu} = \varepsilon^{\frac{3}{2}\mu-1} = o(1) \quad \text{as} \quad \varepsilon \rightarrow 0 \quad \text{or} \quad \mu > \frac{2}{3}. \quad (17)$$

This constitutes our main result:

For any stratifications weaker than $d\bar{\theta}/dz = O(\varepsilon^{2/3})$, the internal wave dynamics of the compressible, pseudo-incompressible, and anelastic models should remain asymptotically close in terms of the flow Mach number *over advective time scales*. This is a considerable improvement over the original Ogura & Phillips' condition for the validity of their anelastic model which requires that $d\bar{\theta}/dz = O(\varepsilon^2)$. For $\varepsilon \sim 1/30$ the Ogura & Phillips' estimate amounts to potential temperature variations of the order of $\Delta\theta|_0^{h_{\text{sc}}} \sim 0.33$ K over the pressure scale height, whereas our new estimate implies validity of the sound-proof models even if

$$\Delta\theta|_0^{h_{\text{sc}}} \sim \theta_{\text{ref}} h_{\text{sc}} \cdot \frac{1}{\theta^*} \frac{d\theta^*}{dz^*} = T_{\text{ref}} \frac{1}{\theta} \frac{d\theta}{dz} \sim 300 \text{ K} \cdot (1/30)^{2/3} \sim 30 \text{ K}, \quad (18)$$

where the asterisc denotes dimensional quantities.

Another indication that at the threshold of $\mu = 2/3$ the dynamics changes non-trivially arises as follows: When $\mu = 2/3$ we have $\nu := 1 - \mu/2 = \mu$, so that the leading nonlinearities on the r.h.s of (16), which are $O(\varepsilon^\nu)$, become comparable to the perturbation terms of the

linearized system on the l.h.s of (16), which are $O(\varepsilon^\mu)$. Thus, for $\mu \leq 2/3$ any perturbation analysis of internal waves in compressible flows that go beyond the leading-order solution must necessarily account for nonlinear effects.

Notice that there is no noticeable transition or change in the structure of the linear eigenmodes and eigenvalues considered in the next section as μ decreases below the threshold of $\mu = 2/3$. The importance of this threshold is associated entirely with the more subtle effects just explained.

The present estimates rely on the linearized equations. But, since all three models considered feature the same leading nonlinearities represented by the nonlinear advection of potential temperature and velocity in (16)_{1,2} (see the terms of order $O(\varepsilon^\nu)$), we expect asymptotic agreement of the solutions over advective time scales as long as the fast linearized dynamics do not already lead to leading-order deviations between the model results, i.e., as long as $\mu > 2/3$. A mathematically rigorous proof of the validity of the fully nonlinear pseudo-incompressible, and possibly the anelastic, models over advective time scales is work in progress.

c. Vertical mode decomposition and the Sturm-Liouville eigenvalue problem

Here we summarize the analysis of internal wave vertical eigenmodes for the three flow models. For simplicity, we assume rigid-wall top and bottom boundaries at $z = 0$ and $z = H = O(1)$, respectively, and seek horizontally travelling waves described by

$$\left(\tilde{\theta}, \tilde{\mathbf{u}}, \tilde{w}, \pi^*\right)(\vartheta, \mathbf{x}, z) = \left(\check{\theta}, \check{\mathbf{u}}, \check{w}, \check{\pi}\right)(z) \exp(i[\omega\vartheta - \boldsymbol{\lambda} \cdot \mathbf{x}]) . \quad (19)$$

Inserting this ansatz into (16), neglecting the nonlinearities, and eliminating $\check{\theta}$, $\check{\mathbf{u}}$, and $\check{\pi}$ we obtain a Sturm-Liouville-type second order differential equation for a suitable vertical velocity structure function $W(z)$,

$$-\frac{d}{dz} \left(\frac{1}{\boldsymbol{\lambda}^2 - A \varepsilon^\mu / \Lambda \bar{c}^2} \phi_{BC} \frac{dW}{dz} \right) + \phi_{BC} W = \Lambda (N^2 \phi_{BC}) W \quad (20)$$

with boundary conditions

$$W(0) = W(H) = 0. \quad (21)$$

Here we have used the following abbreviations:

$$\phi_{BC} = \frac{\bar{\theta}^C}{\bar{\theta}^B} \bar{P}, \quad \bar{c}^2 = \frac{\gamma \bar{P}}{\bar{\rho}}, \quad N^2 = \frac{1}{\bar{\theta}} \frac{d\bar{\Theta}}{dz}, \quad (22)$$

and

$$\Lambda = \frac{1}{\omega^2}, \quad W = \begin{cases} \bar{P} \check{w} & \text{compressible or pseudo-incompressible} \\ \bar{\rho} \check{w} & \text{anelastic} \end{cases}. \quad (23)$$

See the appendix for details of the derivation, and note that $\bar{\theta}^B, \bar{\theta}^C$ are to be read as “ $\bar{\theta}$ to the power B and C ”, respectively.

For $A = 0$, i.e., for either the anelastic or the pseudo-incompressible model, and for any fixed horizontal wave number vector, $\boldsymbol{\lambda}$, eqs. (20), (21) represent a classical Sturm-Liouville eigenvalue problem, about which the following facts are well-known, Zettl (2005):

- i. There is a sequence of eigenvalues and associated eigenfunctions, $(\Lambda_k^0, W_k^0)_{k=0}^\infty$, with $0 < \Lambda_0^0 < \Lambda_1^0 < \dots$, and $\Lambda_k^0 \rightarrow \infty$ as $k \rightarrow \infty$.
- ii. The $(W_k^0)_{k=0}^\infty$ form an orthonormal basis of a Hilbert space of functions $f : [0, H] \mapsto \mathbb{R}$ with scalar product $\langle U, V \rangle = \int_0^H U (N^2 \phi_{BC}) V dz$. Note that the scalar product, and thus the Hilbert space, are independent of the horizontal wave number $\boldsymbol{\lambda}$.

- iii. The vertical mode number, k , equals the number of zeroes of the associated eigenmodes on the open interval $0 < z < H$ (i.e., excluding the boundary points).

We conclude that the two sound-proof models considered here feature well-defined internal wave modes, one such hierarchy of eigenvalues and vertical structures for each wave number vector, $\boldsymbol{\lambda}$. The only differences in the linearized eigenmodes between the pseudo-incompressible and the present anelastic model consist of the scaling factor of $\bar{\theta} = \bar{P}/\bar{\rho}$ in the definition of the structure function $W(z)$ in (23), and of the slightly different way in which the background potential temperature distribution enters the Sturm-Liouville equation. Specifically,

$$\phi_{BC} = \begin{cases} 1/\bar{\theta}\bar{P} & \text{pseudo-incompressible} \\ \bar{\theta}/\bar{P} & \text{anelastic} \end{cases}. \quad (24)$$

Notice that the compressible and pseudo-incompressible models share the definition of W as well as that of ϕ_{BC} .

d. Asymptotics for the compressible internal wave modes

The eigenvalue–eigenfunction problem for the linearized compressible equations, i.e., (20) and (21) with $A = 1$, is *nonlinear* in the eigenvalue Λ . Here we construct first-order accurate approximations to the *weakly* compressible eigenvalues and eigenfunctions, for which $\boldsymbol{\lambda}^2 \gg \varepsilon^\mu/\Lambda\bar{c}^2$, so that the compressibility term in the denominator of the first term in (20) remains a small perturbation, and we may expand the solution as

$$(\Lambda_k^\varepsilon, W_k^\varepsilon) = (\Lambda_k^0, W_k^0) + \varepsilon^\mu (\Lambda_k^1, W_k^1) + O(\varepsilon^{2\mu}), \quad (25)$$

where the W_k^0 are taken to be the eigenfunctions corresponding to the pseudo-incompressible model.

Notice that there is a set of eigenvalues with $\Lambda = 1/\omega^2 = O(\varepsilon^\mu)$ which correspond to the system's high-frequency acoustic modes. Those will not be considered further in this paper.

The perturbation structure functions $W_k^1(z)$ are then expanded in terms of the leading-order eigenfunction basis, $(W_j^0)_{j=0}^\infty$ so that

$$W_k^1 = \sum_j \psi_{k,j} W_j^0. \quad (26)$$

Inserting (25) in (20) we first find that the leading-order terms of order $O(1)$ cancel identically due to the fact that (Λ_k^0, W_k^0) already solve the eigenvalue problem for $A = 0$ and $B = 1$. At $O(\varepsilon^\mu)$ we have, letting $\phi_{BC} \equiv \phi$ for simplicity of notation,

$$-\frac{d}{dz} \left(\frac{\phi}{\lambda^2} \frac{dW_k^1}{dz} \right) + \phi W_k^1 = \Lambda_k^0 (N^2 \phi) W_k^1 + \Lambda_k^1 (N^2 \phi) W_k^0 + \frac{d}{dz} \left(F \frac{dW_k^0}{dz} \right), \quad (27)$$

where

$$F = \frac{\phi}{\Lambda_k^0 \bar{c}^2 \lambda^4}. \quad (28)$$

Multiplying by W_k^0 , integrating from $z = 0$ to $z = H$, and using the orthonormality from item ii above as well as the fact that W_k^0 is the leading-order eigenfunction with eigenvalue Λ_k^0 , we find that the left-hand side and the first term on the right cancel each other, whereas the remaining two terms yield

$$\Lambda_k^1 = \int_0^H F \left[\frac{dW_k^0}{dz} \right]^2 dz. \quad (29)$$

Similarly we find, after multiplication with W_j^0 for $j \neq k$ and integration,

$$\psi_{k,j}^1 = -\frac{1}{\Lambda_j^0 - \Lambda_k^0} \int_0^H F \frac{dW_k^0}{dz} \frac{dW_j^0}{dz} dz. \quad (30)$$

Due to normalization of the eigenfunctions, it turns out that $\psi_{k,k}^1 = O(\varepsilon^\mu)$, and thus contributes a higher-order correction only.

This determines the first-order perturbations in terms of ε^μ from (25), (26). For a forthcoming companion paper, two of the authors currently work on a rigorous proof that the remainders are actually of order $O(\varepsilon^{2\mu})$ as indicated in (25).

Remark: If $\Lambda_j[p, q, r]$ is a simple eigenvalue of a Sturm Liouville operator $L[p, q, r]$ on $[0, 1]$, i.e., if there exists a unique eigenfunction W_j such that $L[p, q, r]W_j = -(pW_j)' + qW_j = r\Lambda_jW_j$ with $W_j(0) = W_j(1) = 0$, then $\Lambda_j[p, q, r]$ depends analytically on the functions p and q in a neighborhood of the coefficients. The derivative of the eigenvalue Λ_j and eigenvector W_j are given by the expressions in (29), (30), (see Kato 1995; Kong and Zettl 1996).

e. Examples

Here we evaluate the leading and first-order results for a background potential temperature distribution

$$\bar{\theta}(z) = (1 - 0.1z)^{-1} \quad (0 \leq z \leq 1.5). \quad (31)$$

With $h_{sc} = p_{ref}/\rho_{ref}g \sim 8.8$ km and $T_{ref} = 300$ K the potential temperature distribution from Fig. 1 results, showing a vertical variation of about 40 K over ~ 13 km. The maximum relative deviation between $\bar{P} = \bar{p}^{\frac{1}{\gamma}}$ and \bar{p} amounts to 15% in this example.

For the present hydrostatic background and horizontal wave numbers $\lambda = 0.5, 2.0, 8.0$, corresponding to horizontal wavelengths of 110.6 km, 27.6 km, and 6.9 km, respectively, the eigenvalues for the compressible and sound-proof systems deviate from each other by less than one percent. Figure 2 shows the leading-order relative difference between the Sturm-

Liouville eigenvalues for the pseudo-incompressible and anelastic models on the one hand, and first-order approximations of the eigenvalues for the compressible model on the other hand. The approximate eigenvalues for the compressible case have been computed here from the first iterate of a Picard iteration in terms of Λ in (20), i.e., from the perturbed regular Sturm-Liouville equation

$$-\frac{d}{dz} \left(\frac{1}{\boldsymbol{\lambda}^2 - A \varepsilon^\mu / \Lambda_k^0 \bar{c}^2} \phi \frac{dW}{dz} \right) + \phi W = \Lambda^1 (N^2 \phi) W . \quad (32)$$

The resulting Λ_k^1 equals the compressible eigenvalue of mode number k up to errors of order $O(\varepsilon^{2\mu})$ as shown rigorously by two of the authors in a forthcoming paper. The $\Lambda_j^1(k)$ for $j \neq k$ resulting from (32) have no physical meaning.

We observe that the relative deviation of the eigenvalues between the sound-proof and compressible cases is surprisingly small in practice. According to our previous analysis, we would expect deviations of the same order of magnitude as the relative vertical variation of the potential temperature, which in the present case is $\varepsilon^\mu \sim 0.1$. Yet, the maximum deviation between the eigenvalues is less than 0.01 for the cases documented in Fig. 2 for mode number $k = 0$, and it even decreases rapidly for larger k . The situation is very similar for other horizontal wave numbers (not shown).

The deviations in the vertical structure functions are similarly small as demonstrated in an exemplary fashion by the differences in the vertical velocity structure functions, $\check{w}_{10}^1 - \check{w}_{10}^0$ for $|\boldsymbol{\lambda}| = 0.5$ and $|\boldsymbol{\lambda}| = 8.0$ in Fig. 3

f. The long-wave limit

Considering (20), one may wonder whether compressibility will play less of a subordinate role for large-scale internal gravity waves with $|\boldsymbol{\lambda}| \ll 1$, as in this case the two terms in the denominator, $\boldsymbol{\lambda}^2 - \varepsilon^\mu / \Lambda \bar{c}^2$, could become comparable. That this is not the case becomes clear after multiplication of the entire equation (20) by $\boldsymbol{\lambda}^2$ and considering the rescaled eigenvalue $\Lambda^*(\boldsymbol{\lambda}) = \boldsymbol{\lambda}^2 \Lambda$. The Sturm-Liouville equation for this variable then reads,

$$-\frac{d}{dz} \left(\frac{1}{1 - \varepsilon^\mu / \Lambda^*(\boldsymbol{\lambda}) \bar{c}^2} \phi \frac{dW}{dz} \right) + \boldsymbol{\lambda}^2 \phi W = \Lambda^*(\boldsymbol{\lambda}) (N^2 \phi) W. \quad (33)$$

As $\boldsymbol{\lambda}^2$ vanishes, the equation approaches a well-defined limit in which second term on the left vanishes asymptotically, and the term $\varepsilon^\mu / \Lambda^* \bar{c}^2$ remains a small perturbation in the denominator of the second-derivative term. As a consequence, the long-wave limiting behavior of the original eigenvalues will be

$$\boldsymbol{\lambda}^2 \Lambda_k \rightarrow \Lambda_k^*(0) \quad \text{as} \quad |\boldsymbol{\lambda}| \rightarrow 0, \quad (34)$$

where $\Lambda_k^*(0)$ is an eigenvalue of the limit problem,

$$-\frac{d}{dz} \left(\frac{1}{1 - \varepsilon^\mu / \Lambda^*(\boldsymbol{\lambda}) \bar{c}^2} \phi \frac{dW}{dz} \right) = \Lambda^*(\boldsymbol{\lambda}) (N^2 \phi) W \quad (35)$$

with the same rigid-wall boundary conditions.

5. Conclusions

In this paper we have addressed the formal asymptotics of weakly compressible atmospheric flows involving three asymptotically different time scales for sound, internal waves,

and advection. Both the pseudo-incompressible and a particular anelastic model yield very good approximations to the linearized internal wave dynamics in a compressible flow for realistic background stratifications and on length scales comparable to the pressure and density scale heights. These sound-proof models should be applicable for stratification strengths $(h_{\text{sc}}/\bar{\theta})(d\bar{\theta}/dz) < O(\varepsilon^{2/3})$, where ε is the flow Mach number. This constraint guarantees the sound-proof and compressible internal waves to evolve asymptotically closely even over advective time scales. For typical flow Mach numbers $\varepsilon \sim 1/30$, this amounts to vertical variations of the mean potential temperature over the pressure scale height of $\Delta\bar{\theta} \sim 30$ K. Considering that $h_{\text{sc}} \sim 8.8$ km for $T_{\text{ref}} = 300$ K and that typical tropospheric heights are about 10...15 km, the estimate for the validity of the sound-proof models yields realistic potential temperature variations of $\delta\bar{\theta} \sim 30$...50 K across the troposphere. We have thus provided an explicit estimate for the regime of validity of the considered sound-proof models that considerably extends Ogura & Phillips' original estimate which required $(h_{\text{sc}}/\bar{\theta})(d\bar{\theta}/dz) = O(\varepsilon^2)$ and implied unrealistically weak background stratifications.

Interesting open questions which we are currently pursuing are: (i) Could either of the sound-proof models be also justified even for $(h_{\text{sc}}/\bar{\theta})(d\bar{\theta}/dz) = O(1)$, and if so, what are the pertinent flow regimes when linear as well as nonlinear effects are taken into account? See also the discussion in (Davies et al. 2003; Almgren et al. 2006) in this context. (ii) Is there a mathematically rigorous justification of the present formal asymptotic results.

Acknowledgements

R.K. thanks the Johns Hopkins University and the US National Center for Atmospheric Research for hosting him during his 2009 sabbatical leave, the Wolfgang Pauli Institute at Wirtschaftsuniversität Wien for their generous hospitality during an intense week of joint research with D.B., Dr. Veerle Ledoux from Gent University for providing the open source Sturm-Liouville eigen-problem solver “Matlise”, Deutsche Forschungsgemeinschaft for partial support through the MetStröm Priority Research Program (SPP 1276), and through Grant KL 611/14. U.A. and R.K. both thank the Leibniz-Gemeinschaft (WGL) for partial support within their PAKT program. O.K. and R.K. thank Alexander-von-Humboldt Stiftung for partial support of this work through their Friedrich-Wilhelm-Bessel prize program. P.K.S. acknowledges partial support by the DOE award DE-FG02-08ER64535. The National Center for Atmospheric Research is sponsored by the National Science Foundation.

Appendix: Derivation of the Sturm-Liouville eq. (20)

Consider the linearized equation (16), i.e., (16) with the r.h.s. terms set to zero. Let $1 + B\varepsilon^\mu\bar{\Theta} \equiv \bar{\theta}^B$. Then we have

$$\begin{aligned}
 \tilde{\theta}_\vartheta + \tilde{w} \frac{d\bar{\Theta}}{dz} &= 0 \\
 \tilde{\mathbf{u}}_\vartheta + \bar{\theta}^B \nabla \pi^* &= 0 \\
 \tilde{w}_\vartheta - \frac{\tilde{\theta}}{\bar{\theta}} + \bar{\theta}^B \pi_z^* &= 0 \\
 A \varepsilon^\mu \pi_\vartheta^* - C \varepsilon^\mu \frac{\gamma \Gamma \bar{\pi}}{\bar{\theta}} \tilde{w} \frac{d\bar{\Theta}}{dz} + \left(\gamma \Gamma \bar{\pi} \nabla \cdot \tilde{\mathbf{v}} + \tilde{w} \frac{d\bar{\pi}}{dz} \right) &= 0
 \end{aligned} \tag{36}$$

Introduce the vertical mode expansion from (19). Then the first two equations in (36) yield

$$\begin{aligned} i\omega\check{\theta} + \check{w}\frac{d\bar{\Theta}}{dz} &= 0 \\ i\omega\check{\mathbf{u}} - \bar{\theta}^B i\boldsymbol{\lambda}\check{\pi} &= 0 \\ i\omega\check{w} - \frac{\check{\theta}}{\bar{\theta}} + \bar{\theta}^B \frac{d\check{\pi}}{dz} &= 0 \end{aligned} \quad (37)$$

$$A\varepsilon^\mu i\omega\check{\pi} - C\varepsilon^\mu \frac{\gamma\Gamma\bar{\pi}}{\bar{\theta}} \check{w} \frac{d\bar{\Theta}}{dz} + \gamma\Gamma\bar{\pi} \left(-i\boldsymbol{\lambda}\cdot\check{\mathbf{u}} + \frac{d\check{w}}{dz} \right) + \check{w} \frac{d\check{\pi}}{dz} = 0$$

Eliminate $\check{\mathbf{u}}$ from the fourth equation in (37) using the second equation in (37) to obtain

$$i \left(A\varepsilon^\mu \omega - \gamma\Gamma\bar{\pi}\bar{\theta}^B \frac{\boldsymbol{\lambda}^2}{\omega} \right) \check{\pi} + \left(\left[\frac{d\check{\pi}}{dz} - \varepsilon^\mu C \frac{\gamma\Gamma\bar{\pi}}{\bar{\theta}} \frac{d\bar{\Theta}}{dz} \right] \check{w} + \gamma\Gamma\bar{\pi} \frac{d\check{w}}{dz} \right) = 0. \quad (38)$$

Use (37)_{1,3} to obtain

$$i \frac{d\check{\pi}}{dz} = \frac{\omega}{\bar{\theta}^B} \left(1 - \frac{N^2}{\omega^2} \right) \check{w} \quad \text{where} \quad N^2 \equiv \frac{1}{\bar{\theta}} \frac{d\bar{\Theta}}{dz}, \quad (39)$$

then solve (38) for $\check{\pi}$, take the z -derivative, and eliminate $i d\check{\pi}/dz$ using (39). This yields, after division by ω ,

$$\frac{1}{\bar{\theta}^B} \left(1 - \frac{N^2}{\omega^2} \right) \check{w} - \frac{d}{dz} \left[\frac{1}{\boldsymbol{\lambda}^2 - A\varepsilon^\mu \omega^2 / \bar{c}^2} \frac{1}{\bar{\theta}^B} \left(\frac{\check{w}}{\gamma\Gamma\bar{\pi}} \frac{d\check{\pi}}{dz} - \varepsilon^\mu C \frac{\check{w}}{\bar{\theta}} \frac{d\bar{\Theta}}{dz} + \frac{d\check{w}}{dz} \right) \right] = 0 \quad (40)$$

where we have used

$$\bar{c}^2 = \frac{\gamma\bar{P}}{\bar{\rho}} = \frac{\gamma\bar{P}\bar{\theta}}{\bar{P}^{1/\gamma}} = \gamma\Gamma\bar{\pi}\bar{\theta}, \quad (41)$$

the definition of $\bar{\pi}$ in (8), and the fact that, according to eqn. (16) and Table 2, we have $\bar{\theta}^B \equiv \bar{\theta}$ whenever $A \neq 0$. Realize that

$$\left(\frac{\check{w}}{\gamma\Gamma\bar{\pi}} \frac{d\check{\pi}}{dz} - \varepsilon^\mu C \frac{\check{w}}{\bar{\theta}} \frac{d\bar{\Theta}}{dz} + \frac{d\check{w}}{dz} \right) = \frac{\bar{\theta}^C}{\bar{P}} \frac{d}{dz} \left(\frac{\bar{P}}{\bar{\theta}^C} \check{w} \right), \quad (42)$$

which, given $\bar{P} = (\Gamma\bar{\pi})^{1/\gamma\Gamma}$ from (8), is obvious for $C = 0$, and follows from $\bar{\theta}(z) = 1 + \varepsilon^\mu \bar{\Theta}(z)$ for $C = 1$. Letting $\bar{\rho}_C = \bar{P}/\bar{\theta}^C$, $W = \bar{\rho}_C \check{w}$, $\phi_{BC} = \bar{\theta}^C / \bar{\theta}^B \bar{P}$, and $\Lambda = 1/\omega^2$ we collect (40)–

(42) to obtain the Sturm-Liouville equation from (20):

$$-\frac{d}{dz} \left[\frac{\phi_{BC}}{\lambda^2 - A\varepsilon^\mu/\Lambda\bar{c}^2} \frac{dW}{dz} \right] + \phi_{BC} W = \Lambda (\phi_{BC} N^2) W \quad (43)$$

where

$$\phi_{BC} = \frac{\bar{\theta}^C}{\bar{\theta}^B \bar{P}} = \begin{cases} \frac{\bar{\theta}}{\bar{P}} & \text{anelastic} \\ \frac{1}{\bar{\theta} \bar{P}} & \text{compressible \& pseudo-incompressible} \end{cases} . \quad (44)$$

REFERENCES

- Almgren, A. S., J. B. Bell, C. A. Rendleman, and M. Zingale, 2006: Low mach number modeling of type ia supernovae. i. hydrodynamics. *The Astrophysical Journal*, **637**, 922–936.
- Bannon, P. R., 1996: On the anelastic approximation for a compressible atmosphere. *Journal of the Atmospheric Sciences*, **53**, 3618–3628.
- Davies, T., A. Staniforth, N. Wood, and J. Thuburn, 2003: Validity of anelastic and other equation sets as inferred from normal-mode analysis. *Q. J. R. Meteorol. Soc.*, **129**, 2761–2775.
- Durran, D. R., 1989: Improving the anelastic approximation. *Journal of the Atmospheric Sciences*, **46**, 1453–1461.
- Dutton, J. A. and G. H. Fichtl, 1969: Approximate equations of motion for gases and liquids. *Journal of the Atmospheric Sciences*, **47**, 1794–1798.
- Kato, T., 1995: *Perturbation theory for linear operators*. Classics in Mathematics, Springer Verlag.
- Klein, R., 2009: Asymptotics, Structure, and Integration of Sound-Proof Atmospheric flow Equations. *Theoretical and Computational Fluid Dynamics*, **23**, 161–195.

- Kong, Q. and A. Zettl, 1996: Eigenvalues of regular sturm-liouville problems. *J. Differential Equations*, **131**, 1–19.
- Lipps, F. and R. Hemler, 1982: A scale analysis of deep moist convection and some related numerical calculations. *Journal of the Atmospheric Sciences*, **29**, 2192–2210.
- Ogura, Y. and N. A. Phillips, 1962: Scale analysis of deep moist convection and some related numerical calculations. *Journal of the Atmospheric Sciences*, **19**, 173–179.
- Prusa, J., P. Smolarkiewicz, and A. Wyszogrodzki, 2008: Eulag, a computational model for multiscale flows. *Computers & Fluids*, **37**, 1193–1207.
- Zettl, A., 2005: *Sturm-Liouville Theory*, Math. Surveys & Monographs, Vol. 121. American Mathematical Society.

List of Tables

1	Characteristic inverse time scales	27
2	Switching parameters in eqn. (16).	28

TABLE 1. Characteristic inverse time scales

	dimensional	dimensionless
advection	$\frac{u_{\text{ref}}}{h_{\text{sc}}}$	1
internal waves	$N = \sqrt{\frac{g}{\bar{\theta}} \frac{d\bar{\theta}}{dz}}$	$\frac{\sqrt{gh_{\text{sc}}}}{u_{\text{ref}}} \sqrt{\frac{h_{\text{sc}}}{\bar{\theta}} \frac{d\bar{\theta}}{dz}} = \frac{1}{\varepsilon} \sqrt{\frac{h_{\text{sc}}}{\bar{\theta}} \frac{d\bar{\theta}}{dz}}$
sound	$\frac{\sqrt{gh_{\text{sc}}}}{h_{\text{sc}}}$	$\frac{\sqrt{gh_{\text{sc}}}}{u_{\text{ref}}} = \frac{1}{\varepsilon}$

TABLE 2. Switching parameters in eqn. (16).

model	A	B	C
compressible	1	1	0
pseudo-incompressible	0	1	0
anelastic	0	0	1

List of Figures

- 1 Sample potential temperature distribution (left) and the resulting dimensionless vertical distributions of $\bar{P} = \bar{\rho}\bar{\theta}$ and $\bar{\rho}$. 30
- 2 Comparison between the sound-proof and first-order accurate approximations to the compressible internal wave eigen-values for the background state from Fig. 1 and horizontal wave numbers $|\boldsymbol{\lambda}| = 0.5$ (a), $|\boldsymbol{\lambda}| = 2.0$ (b), and $|\boldsymbol{\lambda}| = 8.0$ (c). The approximate compressible eigenvalues and eigenmodes are defined through the perturbed Sturm-Liouville problem in (32). The graph shows relative differences of the eigenvalues $(\Lambda_j^0 - \Lambda_j^1)/\Lambda_j^0$. 31
- 3 Vertical velocity structure functions for the same case as in Fig. 2 and mode number $k = 10$ and horizontal wave numbers $|\boldsymbol{\lambda}| = 0.5$ (top row) and $|\boldsymbol{\lambda}| = 8.0$ (bottom row). Structure functions (left) and their deviations of the sound-proof modes from the first-order accurate compressible mode (right). 32

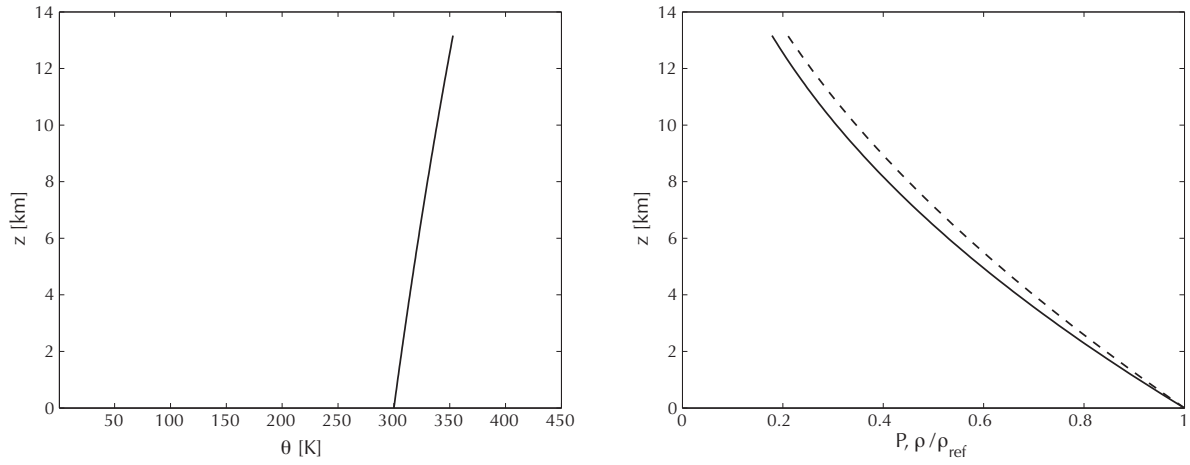
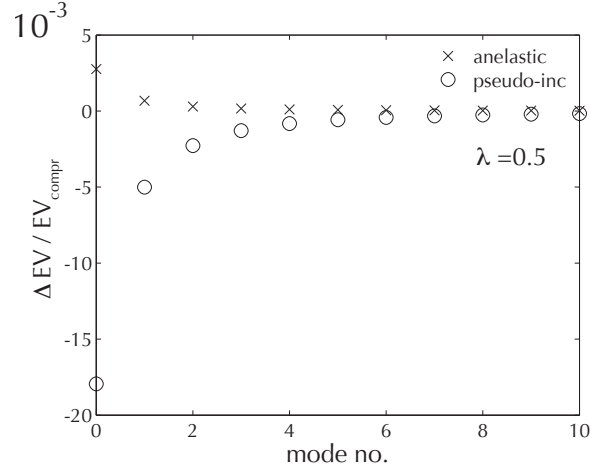
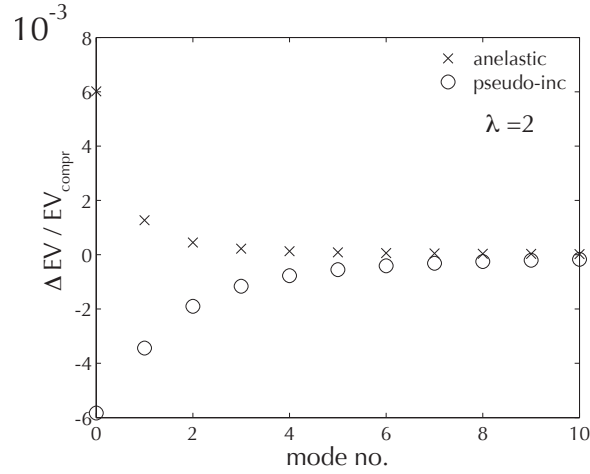


FIG. 1. Sample potential temperature distribution (left) and the resulting dimensionless vertical distributions of $\bar{P} = \bar{\rho}\bar{\theta}$ and $\bar{\rho}$.

a) $L = 110$ km



b) $L = 27.6$ km



c) $L = 6.9$ km

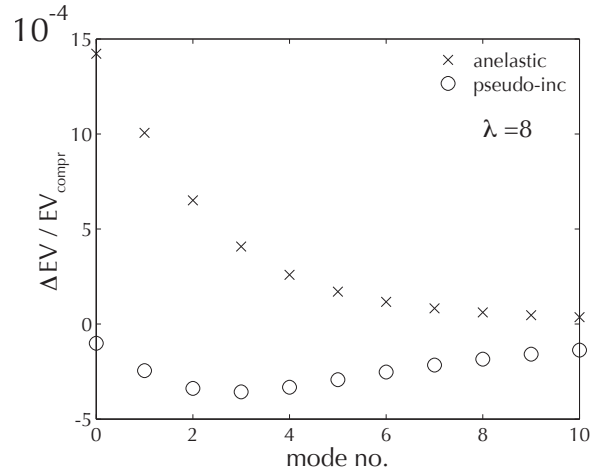


FIG. 2. Comparison between the sound-proof and first-order accurate approximations to the compressible internal wave eigen-values for the background state from Fig. 1 and horizontal wave numbers $|\boldsymbol{\lambda}| = 0.5$ (a), $|\boldsymbol{\lambda}| = 2.0$ (b), and $|\boldsymbol{\lambda}| = 8.0$ (c). The approximate compressible eigenvalues and eigenmodes are defined through the perturbed Sturm-Liouville problem in (32). The graph shows relative differences of the eigenvalues $(\Lambda_j^0 - \Lambda_j^1)/\Lambda_j^0$.

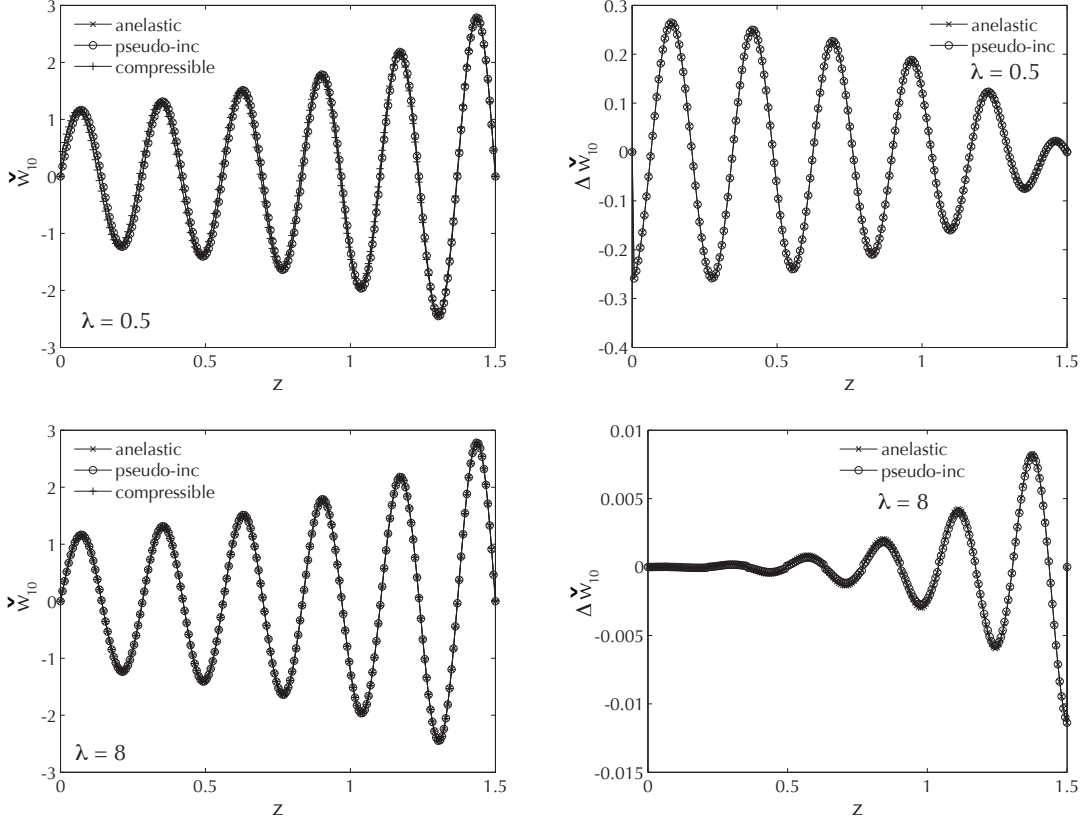


FIG. 3. Vertical velocity structure functions for the same case as in Fig. 2 and mode number $k = 10$ and horizontal wave numbers $|\lambda| = 0.5$ (top row) and $|\lambda| = 8.0$ (bottom row). Structure functions (left) and their deviations of the sound-proof modes from the first-order accurate compressible mode (right).